An Evaluation of Millimeter-wave Radar Sensing for Civil Infrastructure

Daniel Mitchell
Smart Systems Group (SSG)
Heriot-Watt University
Edinburgh, United Kingdom
Daniel.Mitchell@hw.ac.uk

Jamie Blanche
Smart Systems Group (SSG)
Heriot-Watt University
Edinburgh, United Kingdom
j.blanche@hw.ac.uk

David Flynn
Smart Systems Group (SSG)
Heriot-Watt University
Edinburgh, United Kingdom
d.flynn@hw.ac.uk

***Abstract*—Critical infrastructure is a dense network of systems that provide vital services such as energy, transport and water. Continuous cycles of monitoring and repair are vital to the economic development and functions of a community. Current detection methods of subsurface fault precursors in civil infrastructure are insufficient for subsurface defect detection. In this paper we present the analysis of complex multi-layer structures with radar, Frequency Modulated Continuous Wave (FMCW) sensing. Results have demonstrated the ability of K-band analysis to detect embedded and obscured materials during inspection by detecting contrasts in the return signal amplitude from the sensor. This includes detection of the depth and geometry of subsurface materials and detection of water ingress within materials. Thus, we propose that FMCW analysis represents a novel method of non-invasive, non-contact and non-destructive analysis of dielectric and multi-layer materials applicable to asset integrity and health monitoring for the civil infrastructure sector. This research ensures that inspection engineers have tools available which can provide quantitative and qualitive results enabling more effective assessment of the subsurface integrity of a structure. The FMCW sensing modality provides early prognostics and remedial action to be taken, reducing the downtime of an asset and risk of failure.**

***Keywords*—Data Analytics, Modern Electronic Devices, Non-Destructive Evaluation, Predictive Maintenance, Reinforced Concrete, Structural Health Monitoring**

I. INTRODUCTION

Our economic infrastructure is a complex network of systems providing energy, transport, water, waste management, telecommunications and flood defenses that enable the essential services on which our society depends. An effective infrastructure requires a cyclic integration of activities; design, construction, inspection, repair, maintenance, renewal and upgrading to satisfy ever-increasing societal requirements for connectivity, mobility and access to resources that underpin economic development [1]. In terms of civil infrastructure, Reinforced Concrete (RC) has many benefits for construction. RC is durable, versatile and more fire resistant than other commonly used building materials, enabling safer infrastructure [2]. Premature deterioration of civil infrastructures such as highways, bridges, offshore platforms, pipelines and dams, and is often due to corrosion effects: steel rebar is primarily composed of iron, which significantly compromises the remaining useful life of an asset [3].

The American Road & Transportation Builders Association (ARTBA) reports that 37% of U.S bridges, nearly 231,000 spans, require repair work , with 46,000 bridges which were classified as structurally deficient and recommends that a total of 81,000 bridges be replaced [4]. ARBTA estimated the cost of implementing the identified repairs amount to nearly $164 billion and identified that 178 million motorists access these compromised structures daily. The Federal Highway Administration (FHWA) is responsible for supporting state highway agencies with the design, construction, and maintenance of the U.S highway system [4–6].

RC structures deteriorate due to climate and external elements such as freeze-thaw damage. Hydration of cement creates a highly alkaline environment, which provides a passive layer of protection from air and moisture for embedded rebar [7–9]. Without this layer, corrosion of rebar occurs rapidly due to the ingress of aggressive agents. Corrosion of iron rebar is caused by the prolonged exposure to chlorides which penetrate the porous concrete through water by diffusion and absorption reaching the rebar interface. The passive layer can also be reduced by carbonation in a reaction with CO_2 [3], [7], [8].

The combination of both carbonation and chloride-polluted concrete was reported by Tissier *et al.* (2019) , who investigate corrosion repair mechanisms and study electrochemical chloride extraction to reduce the rate of corrosion onset [10]. The use of electrochemical chloride extractions were shown to decrease the rate of corrosion by three orders of magnitude and demonstrated chloride extraction of 90%. Tissier *et al.* (2019) also found that intra-sample pH was increased by these

This work is funded by Engineering Physical Sciences Research Council (EPSRC) Offshore Robotics for the Certification of Assets (ORCA) Hub [EP/R026173/1].

978-1-7281-8416-6/20/$31.00 ©2020 IEEE

methods, ensuring the passive protective layer within RC is maintained.

Ground penetrating radar is applied by Hasan *et al.* (2016) and uses two-way travel time to detect corroded rebar in water-oil; a combination used as a substitute of concrete in geophysical investigation, and established that two-way travel time increases linearly with the increase of rebar corrosion [11]. Mitigation of RC deterioration during the construction phase by use of natural pozzolan is discussed by Fajardo *et al.* (2009) as a 10-20% substitute for cement, exhibiting significant benefits on the effect of corrosion behaviour on steel and higher mortar resistivity [8].

An alternative prevention method uses Hybrid Fibre-Reinforced Concrete (HyFRC) for corrosion mitigation in steel-reinforced concrete. HyFRC is constructed with discontinuous short and long steel fibers dispersed through concrete. The short fibers improve tensile strength and long fibers improve ductility, resulting in a construction material that is damage-tolerant of corrosion-induced cracking and structural loading [9], [12], [13]. This composite improves longevity prior to the onset of corrosion on steel rebar when compared to conventional reinforced concrete. When HyFRC fails under tensile stress, the delay of corrosion is due to the fiber reinforcement preventing the maximum opening of the instigated crack, inhibiting NaCl solution penetration which accelerates corrosion onset [9].

Current Structural Health Monitoring (SHM) systems have a variety of limitations e.g. require a stimulus to the inspected target, direct line sight or physical contact, etc. For example, visual inspections, while fast and inexpensive, are only useful in cases of external surface faults and are subject to interpretation of the human investigator. Acoustic emission has been proven to be an accurate Non-Destructive Evaluation (NDE) tool, but is susceptible to noise, requires physical contact and often needs other NDE methods to verify results [23–25].

Mitigation and prevention of corrosion are major avenues of research in the civil infrastructure Research & Development sector. However, fluid ingress and corrosion will always be factors present in the use of steel and iron rebar in this structural role. Our research aims to augment/compliment these mitigation strategies via the detection of early fault precursors of embedded rebar to ensure the integrity of vital civil infrastructure by reducing risk and operational costs via predictive and proactive corrosion mitigation. This paper presents a unique method of NDE for fault prognosis of iron rebar via the application of patented Frequency Modulated Continuous Wave (FMCW) radar technology [17]. FMCW radar sensing provides early detection of fault precursors as a non-contact, non-invasive inspection method, enabling access to new information about the integrity of a structure. This novel application enables early detection of faults prior to structural deterioration contributing to a gap in asset integrity monitoring. The development and verification of FMCW radar as an NDE tool is demonstrated in these laboratory-based experiments, which examine the Return Signal Amplitude (RSA) of the radar emissions for detection of distinct subsurface material responses and properties, which are not visible externally.

FMCW radar sensing provides early detection of fault precursors as a non-contact, non-invasive inspection method, enabling access to new information about the integrity of a structure. This novel application enables early detection of faults prior to structural deterioration contributing to a gap in asset integrity monitoring

A summary of the capabilities of FMCW sensing for material analysis and as an inspection tool has been summarised by the authors for the X-Band (8 – 12 GHz) and K-band (18 – 26 GHz) [18], [19]. Key applications include the analysis of dynamic load deformation in geomaterials with the potential to predict sample failures [20], FMCW detection of corrosion under insulation and corrosion precursors [21] and the detection of pore-space contents in partially fluid-saturated geomaterials and 3D-printed polymer geomaterial analogues [22], [23]. FMCW in the K-band has also been demonstrated to support object localisation in opaque environments and for safety applications wherein the detection of people concealed by walls provides forewarning of unexpected human incursion within the mission space of autonomous robotic platforms [24]. In addition, other inspection techniques include low frequency sonar analysis of subsea cables with a view to in-situ integrity monitoring of cables [25]. This includes predicting damage and life expectancy of subsea power cables with emphasis in the offshore renewable energy sector [26] [27].

The remainder of this paper is structured as follows; Section II outlines the dielectric theory. Section III presents the methodology and experimental setup of FMCW radar for the inspection of subsurface materials in sand and within sandstone where section III.A describes the methodology for the embedded material analysis of different types of metals buried in sand, section III.B presents the procedure for the embedded material analysis of metals and water ingress within sandstone and section III.C presents the methodology for the analysis of the return signal for different types of sandstone embedded within the sandpit. Section IV presents the results for each experiment where section IV.A.1) presents the results for variations in material burial depth, section IV.A.2) presents the results for variations in material geometry when buried in the sandpit. Within section IV.B the results are presented for the embedded material analysis of obscured metals and water ingress within the Darney sandstone and section IV.C presents the results for embedded material analysis of two types of sandstone which were buried inside the sandpit. The discussion of this paper is presented in section V and section VI concludes.

II. Dielectric Theory

FMCW radar sensing offers a continuous sweep in frequency, which enables key benefits against a single frequency, pulsed radar. These advantages include a broader frequency range, improved signal to noise characteristics, a lower intermediate frequency and more effective immunity to ambient conditions [23].

Dielectric relaxation processes govern wave attenuation and dispersion in all materials as defined by the relative permittivity ε_r^*. Relaxation processes dampen the localised oscillations of constituent materials at differing rates throughout the component scale range due to the frequency of incident radiation. The observed RSA in low dielectric porous materials is affected by many factors, including interfacial geometry, surface contaminants, fluid content and type and the abundance of high permittivity minerals [28]. Previous experimentation focused on the signal response specific to the presence of water and oil within a geomaterial in the X and K-band, capitalizing on the significant attenuation due to heavy absorption by water in the K-band. A full description of FMCW radar interaction between porous media partially saturated with fluids and internal geomaterial properties via non-invasive FMCW measurement is provided by Blanche *et al.* (2018) [23] and Blanche *et al.* (2020) [20].

III. Experimental Setup and Methodology

A. Embedded Material Analysis of Metals in Sand

This experiment evaluates FMCW sensitivity to depth and geometries of multiple metallic targets buried in loosely consolidated sand. The experimental setup is illustrated in Fig. 1. To analyze the RSA for varying target geometry, a copper sheet was compared to a copper rod at the same buried depth. The distance from the sand surface to the antenna was 10 cm throughout the experiment, ensuring that variations in observed RSA were due to the measurands under test: depth, material type and target geometry. Each target shape was placed on the sand surface and at 5 cm, 10 cm and 15 cm depths.

Aluminium, brass, iron and steel were tested for variations in shape and size to establish FMCW sensitivity. The K-Band FMCW radar was set to complete a frequency sweep of 24-25.5 GHz for a chirp duration of 300 milliseconds.

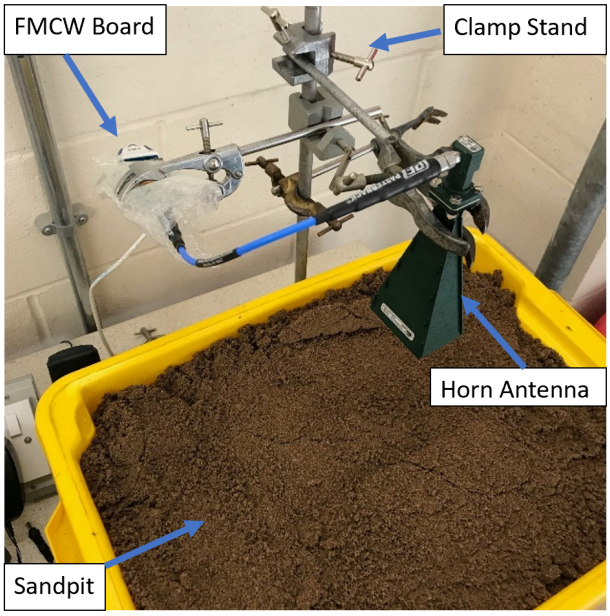

Fig. 1 Experimental setup of sandpit highlighting equipment and target area

B. Embedded Material Analysis of Darney Sandstone

This experiment measures the RSA of the FMCW radar for embedded metals within Darney sandstone. Two 38 mm diameter apertures were cored as shown in Fig. 2, allowing for materials to be placed internally for tests. A metal ruler and a drill bit were then inserted at separate points during the experiment to identify the sensitivity of the FMCW radar to the metals. Lastly, 3ml of water were dropped onto the edge of the aperture, ensuring it was in the target area of the radar. The antenna target separation distance was 10 cm.

C. Embedded Material Analysis of Different Types of Sandstone

This experiment utilises the experimental setup as in section A, where the buried metals were replaced with the Darney sandstone block pictured in Fig. 2 and Lazonby sandstone in Fig. 3. This experiment was conducted to detect the sensitivity of the FMCW radar to the burial of different types of sandstones within the sandpit. Each Darney sandstone was positioned at the bottom of the sandpit and then repeated for the Lazonby sandstone. This experiment was constrained to the depth of the sandpit, therefore allowing for a 3cm layer of sand on top of the embedded material. Additionally, the antenna was positioned to avoid the cored aperture on the Darney sandstone, to ensure consistent and accurate results.

IV. Data Analysis and Results

A. Embedded Material Results of Metals in Sand

The results captured by the FMCW radar are represented as the RSA with absolute units (a.u) in the time frequency domain following a Fast Fourier Transform (FFT). This enables detection of bulk material properties within a porous medium as a function of range from the sensor in air. The FFT is typically used as a range estimation to a target and is expressed as a BIN number, however, this paper establishes that the FFT also reveals key characteristics about material properties [29]. Baseline measurements were taken with no embedded rebar present in the experimental setup. The baseline measurements are displayed within Fig. 4 - 6 as a black double dashed line.

1) Investigation of Depth of Embedded Rebar

These results show that embedded material RSA decreases incrementally as a function of increasing the burial depth. This was observed for the copper sheet (Fig. 4) and copper rod (Fig. 5). This is due to the grains of sand absorbing the signal from the radar, resulting in a direct relationship between the RSA reduction as a function of sand depth. The observed results indicate that the radar sensor is effective as a penetrating radar to detect copper when it is concealed under the sand at different depths.

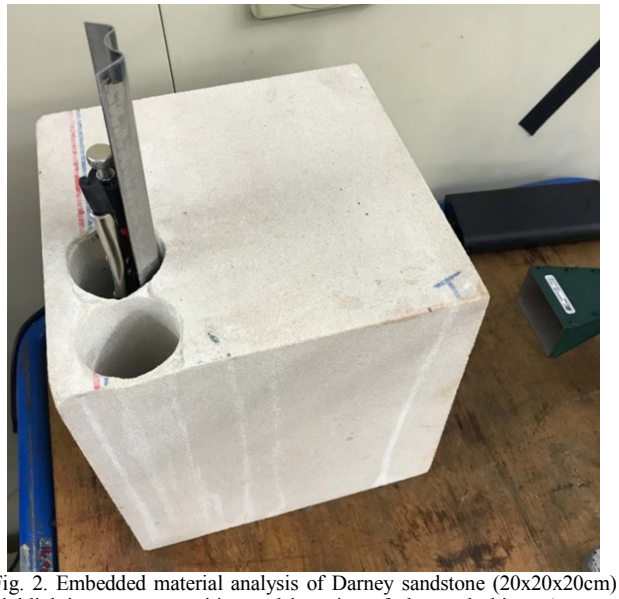

Fig. 2. Embedded material analysis of Darney sandstone (20x20x20cm) highlighting antenna position and insertion of obscured object. Antenna visible to the right of sandstone

Fig. 3. Lazonby Sandstone measuring 20x20x20cm

2) *Investigation of the Shape of Embedded Material*

The RSA of the FMCW radar is shown in Fig. 6 for a copper sheet versus a copper rod. These results show that a copper sheet returns a higher RSA than a copper rod, where the dashed lines for the copper sheet, have a higher RSA at the sample interface than the solid lines with asterisks, representing a copper rod. The RSA is sensitive to target geometry, where a flat metal target reflects more of the incident energy than a cylindrical rod.

B. *Embedded Material Analysis of Darney Sandstone*

This section presents the results for RSA and phase shift for metals and water placed within the Darney sandstone block. A baseline was established for the empty aperture for ~2-minutes, as indicated in Fig. 7 up to point 1. Any observed deviations from this baseline indicate the FMCW sensitivity to the presence of the obscured targets. Table 1 summarizes the results shown in Fig. 7. The hardened steel cylinder drill bit with a diameter of 2cm, was inserted at the rear edge of the aperture, relative to the sensor, where the observed RSA and phase shift increases from the baseline, as indicated at point 1. The hardened steel cylinder drill bit was then repositioned within the aperture to be closer to the antenna. As indicated at point 2, the RSA increases further. A stainless-steel ruler was placed into the aperture, which resulted in a further increase in RSA and large decrease of the phase shift at point 3. The stainless-steel ruler was reoriented within the aperture, resulting in an increase of the RSA and a decrease of the phase shift shown at point 4. The steel ruler and drill bit were then removed from the aperture, where the RSA was observed to return to the baseline. At point 5, 3 ml of water were deposited within the aperture by using a dropper. The observed RSA and phase changes occur gradually as capillary action and gravity cause the water to spread within the sensors field of view. This experiment demonstrates that the FMCW radar sensor is highly sensitive to embedded metals and water ingress within a porous sandstone target.

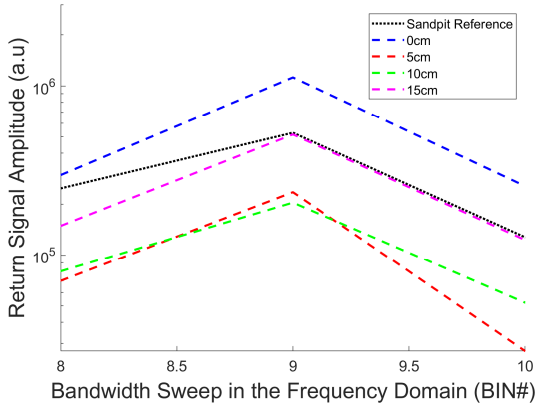

Fig. 4. Return signal amplitude for embedded copper sheet buried at different depths within sandpit

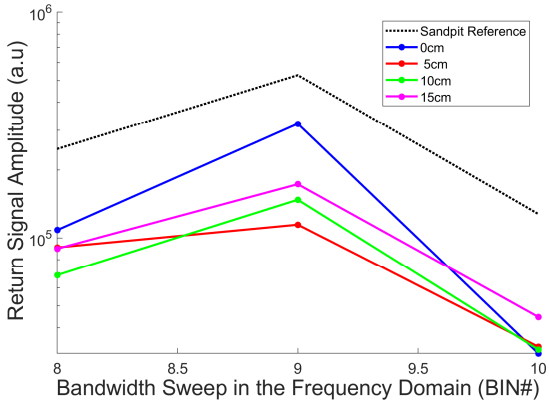

Fig. 5. Return signal amplitude for embedded copper rod buried at different depths within sandpit

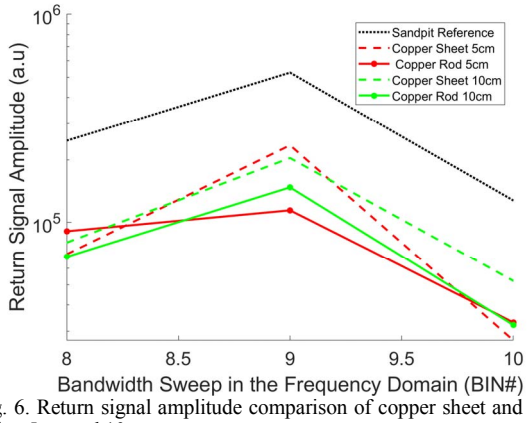

Fig. 6. Return signal amplitude comparison of copper sheet and copper rod at 5cm and 10cm

TABLE 1 DESCRIPTION OF Fig. 7 PROCESS STEPS

Box Number	Description of experimental parameter changed and the resulting return signal analysis
1	Dulled drill bit added in aperture, obscured by sandstone, Return Signal Amplitude (RSA) increases from baseline
2	Dulled drill bit moved closer to sensor but still obscured by sandstone, RSA increases further
3	Stainless steel ruler added in aperture. Large increase in RSA and phase shifts markedly
4	Stainless steel ruler re-orientated in aperture to concave side, RSA increases further and phase shifts
5	Steel ruler and drill bit removed. Water added to wall of aperture, RSA changes dynamically as water seeps into pores, phase shift increases and decreases

C. *Embedded Material Analysis of Different Types of Sandstone*

This section demonstrates that FMCW sensing is sensitive to porous structures which are embedded within a material. The Darney sandstone has a typical porosity of 18.7% and contains relatively well-sorted, sub-angular quartz (SiO_2) grains, of fine to medium grain size (125 – 350 µm), with subsidiary orthoclase feldspar and clay (kaolinite) present within some pore spaces [22], [23]. The Lazonby sandstone has a significantly lower observed porosity at 11.6%, which is considerably lower than the other samples which were previously analyzed by Blanche *et al.* [23]. This is due to the sample being dominated by highly-cemented, grain supported, fine to medium-sized spheroidal, subrounded/rounded grains and well-sorted quartz clasts, ranging between 200-500 µm. The Lazonby sample contains mainly quartz and orthoclase feldspar with some clays with very much the same proportions as the Darney sandstone. However, the iron content is more dispersed throughout Lazonby when compared to Darney sandstone, although the magnitude is similar. Fig. 8 highlights a distinct RSA for the Darney sandstone against the Lazonby sandstone, enabling FMCW detection and characterization of subsurface and embedded materials.

V. DISCUSSION

This research demonstrates the sensitivity of FMCW radar inspection to key asset integrity measurands and validates millimetre-wave sensing as a novel and effective tool for the detection of subsurface properties of obscured defects in static and dynamic conditions. Detection of embedded rebar analogues of differing shape and depths within sand, show that the FMCW sensor may identify a distinct RSA for each scenario within a simulated infrastructural asset. This research establishes FMCW sensitivity to obscured metals and trace

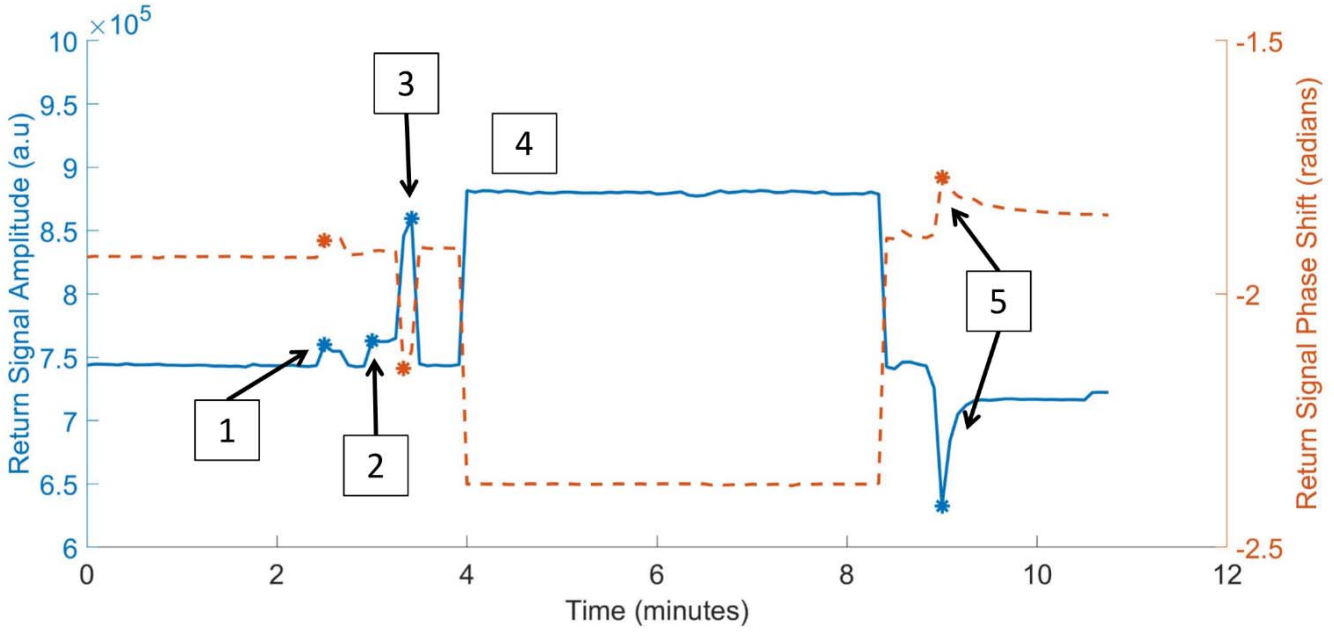

Fig. 7 The return signal amplitude and return signal phase shift (ϕ) against time in minutes

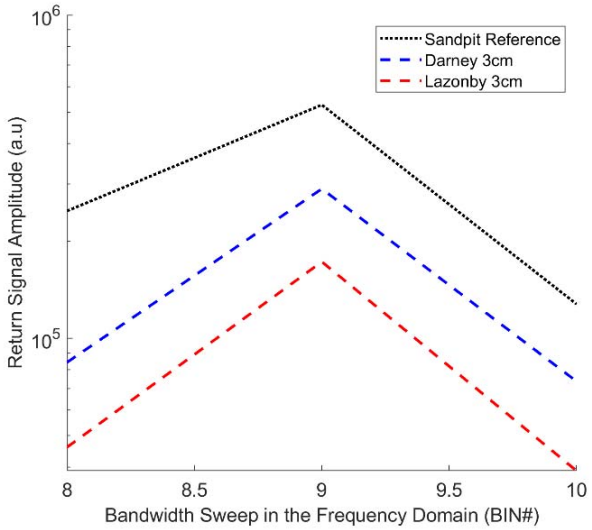

Fig. 8. Return signal amplitude comparison of sandpit reference, Darney sandstone and Lazonby sandstone

volumes of water ingress, acting as a precursor to corrosion onset.

The FMCW radar sensor also successfully demonstrated sensitivity to the differentiation of similar sandstone materials. This novel NDE method represents a useful tool for inspection engineers for the detection of differing types of subsurface and embedded materials when assessing the internal integrity of a structure.

Fig. 4 and Fig. 5 display a similar discrepancy for the RSA at a depth of 15cm. This could be due to an accumulation of water vapor within the sandpit due to atmospheric humidity as the experiment was run over a two-day period for various samples. Further work to evaluate this discrepancy will include heating the sand between experiments to remove any humidity.

The FHWA estimated the cost of replacement and repair of 46,155 structurally deficient bridges across the U.S to be $51.4 billion [30]. The development of non-contact and non-destructive surveying will be key to the evolution of future inspection methods to ensure the holistic safety of infrastructure and hidden defect identification. FMCW radar offers significant benefits such as real-time detection of porous structures allowing accurate location of sub-surface defects before degradation in structural integrity reaches criticality.

The development of Robotic and Autonomous Systems (RAS) has an important role to play in the improvement of asset integrity management. Mobile robotics with flexible sensors will improve decisions of engineers due to data-driven information for scheduled condition monitoring of infrastructure [31]. RAS addresses other challenges by removing humans from dangerous operations such as working from height or within confined spaces. The equipment used for the FMCW radar sensor is low power, designed to military specifications of shock and load resilience and can be integrated into existing systems. The equipment is lightweight and has been integrated with Unmanned Aerial Vehicles (UAVs) and other service robotics for fault prognosis and infrastructural health management roles.

Further work will address detection of embedded iron rebar for varying degrees of corrosion. A library of faults will be established within the database of the sensor for detection of subsurface faults within materials, in addition to detection of subsurface cracking and other subsurface fault precursors which could rapidly cause a structure to deteriorate and become unsafe.

Due to the low dielectric material penetration capability identified in this research, the FMCW system has the potential to be used as a non-destructive tool for the detection of salt and pothole precursors on roads. The measurement of residual salt on road surfaces is not currently applied when spreading salt. Therefore, there is potential to reduce the expenditure on salt as gritters often spread excessive volumes of salt on roads to compensate for significant uncertainties in residual salt levels and ensure they are safe to use. In addition, potholes are a common problem, where repair strategies are enacted only once significant deterioration has occurred. If pothole precursors could be identified prior to significant degradation, this would enable a safer transport network with minimal disruption. Potholes are common around the UK due to the freeze and thaw of water underneath the surface. Future work will consist of developing the sensor to detect other civil infrastructural problems which include bridges, buildings and road maintenance. This includes pothole precursors to ensure roads can be maintained early before significant deterioration alongside salt residue detection.

This work will also be displayed within a digital twin in the future, which acts as a database for engineers where faults can be accessed, monitored and managed with guidelines, advising priority of repair work and remaining useful life. Digital twins are a rapidly growing technology which will be crucial for asset management of structures and assets as it enables inspection engineers to view a complete overview of a system or plant, including history of maintenance, scheduled maintenance and predicted maintenance in the future. In addition, as RAS begin to be integrated into inspection mechanisms, the digital twin will act as a tool for robotic operators to assess the integrity of their robot fleets as these platforms will be seamlessly providing self-certification and safety compliance data to the operator. Therefore, enabling trusted autonomy as the robotic platform can distinguish if it is operational or needs maintenance.

VI. Conclusion

The structural integrity of civil infrastructural assets is imperative to all sectors charged with ensuring the built environment remains safe. The application of this research offers early detection of fault precursors of embedded steel rebar to verify the integrity of vital civil infrastructure, with the potential to ascertain the integrity of the wider civil infrastructural networks of roads and bridges, in addition to building integrity. This research will allow for more accurate

inspections and acquired data to inform the remaining useful life of an asset, with repair work performed earlier and prior to significant structural degradation and prevent disruption of vital societal networks. This enables an asset to remain operational for longer, with predictable and schedulable downtime, maximizing efficiency and safety.

ACKNOWLEDGMENT

The research within this paper has been supported by the Offshore Robotics for Certification of Assets (ORCA) Hub [EP/R026173/1] and the authors wish to thank MicroSense Technologies Ltd for use of their patented FMCW radar sensor (PCT/GB2017/053275).

REFERENCES

[1] UK-RAS, "Robotic and Autonomous Systems for Resilient Infrastructure," 2017, Accessed: Jun. 05, 2020. [Online]. Available: www.ukras.org.

[2] B. Mosley, J. Bungey, and R. Hulse, *Reinforced concrete design to Eurocode 2*, 7th ed. Basingstoke: Palgrave Macmillan, 2012.

[3] F. Tang, G. Chen, R. K. Brow, J. S. Volz, and M. L. Koenigstein, "Corrosion resistance and mechanism of steel rebar coated with three types of enamel," *Corros. Sci.*, vol. 59, 2012, doi: https://doi.org/10.1016/j.corsci.2012.02.024.

[4] American Road & Transportation Builders Association (ARTBA), "2020 Bridge Report," 2020.

[5] "About the Federal-aid Highway Program - Federal-aid Essentials for Local Public Agencies." https://www.fhwa.dot.gov/federal-aidessentials/federalaid.cfm.

[6] "About | Federal Highway Administration." https://www.fhwa.dot.gov/about/.

[7] "The Repair of Reinforced Concrete - John Broomfield." https://www.buildingconservation.com/articles/concrete/concrete.htm.

[8] G. Fajardo, P. Valdez, and J. Pacheco, "Corrosion of steel rebar embedded in natural pozzolan based mortars exposed to chlorides," *Constr. Build. Mater.*, vol. 23, Feb. 2009, doi: 10.1016/j.conbuildmat.2008.02.023.

[9] W. Nguyen, J. F. Duncan, T. M. Devine, and C. P. Ostertag, "Electrochemical polarization and impedance of reinforced concrete and hybrid fiber-reinforced concrete under cracked matrix conditions," *Electrochim. Acta*, vol. 271, pp. 319–336, 2018, doi: https://doi.org/10.1016/j.electacta.2018.03.134.

[10] Y. Tissier, V. Bouteiller, E. Marie-Victoire, S. Joiret, T. Chaussadent, and Y. Tong, "Electrochemical chloride extraction to repair combined carbonated and chloride contaminated reinforced concrete," *Electrochim. Acta*, vol. 317, 2019, doi: https://doi.org/10.1016/j.electacta.2019.05.165.

[11] M. I. Hasan and N. Yazdani, "An Experimental Study for Quantitative Estimation of Rebar Corrosion in Concrete Using Ground Penetrating Radar," *J. Eng.*, vol. 2016, 2016, doi: http://dx.doi.org/10.1155/2016/8536850.

[12] I. Markovic, "High-Performance Hybrid-Fibre Concrete-Development and Utilisation," Delft University of Technology, 2006.

[13] V. Marcos-Meson, A. Michel, A. Solgaard, G. Fischer, C. Edvardsen, and T. L. Skovhus, "Corrosion resistance of steel fibre reinforced concrete - A literature review," *Cem. Concr. Res.*, vol. 103, pp. 1–20, 2018, doi: https://doi.org/10.1016/j.cemconres.2017.05.016.

[14] C. U. Grosse, "Acoustic emission (AE) evaluation of reinforced concrete structures," in *Non-Destructive Evaluation of Reinforced Concrete Structures: Non-Destructive Testing Methods*, Elsevier Inc., 2010, pp. 185–214.

[15] E. M. Charalampidou, S. A. Hall, S. Stanchits, G. Viggiani, and H. Lewis, "Shear-enhanced compaction band identification at the laboratory scale using acoustic and full-field methods.," . *Int. J. Rock Mech. Min. Sci.*, vol. 67, pp. 240–252, 2014.

[16] G. Kwiatek, E. M. Charalampidou, G. Dresen, and S. Stanchits, "An improved method for seismic moment tensor inversion of acoustic emissions through assessment of 2 sensors' coupling and sensitivity to incidence angle.," *2014*, p. 3.

[17] M. P. Y. Desmulliez, S. K. Pavuluri, and G. Goussettis, "Sensor System for Detection of Material Properties," WO 2018/078401, 2018.

[18] J. Blanche, D. Flynn, H. Lewis, G. D. Couples, and R. Cheung, "Analysis of geomaterials using frequency modulated continuous waves," *13th International Conference on Condition Monitoring and Machinery Failure Prevention Technologies 2016*. 2016, [Online]. Available: http://www.scopus.com/inward/record.url?scp=85002836284&partnerID=8YFLogxK.

[19] J. Blanche, D. Flynn, H. Lewis, G. Couples, and R. Cheung, "Analysis of Geomaterials using Frequency Modulated Continuous Wave Radar in the X-band," *IEEE 26th Int. Syposium Ind. Electron. ISIE*, doi: https://doi.org/10.1109/ISIE.2017.8001446.

[20] J. Blanche, J. Buckman, H. Lewis, D. Flynn, and G. Couples, "Frequency Modulated Continuous Wave Analysis of Dynamic Load Deformation in Geomaterials," 2020, doi: 10.4043/30479-ms.

[21] D. S. Herd, "Microwave Based Monitoring System for Corrosion Under Insulation," 2016.

[22] J. Blanche *et al.*, "Dynamic Fluid Ingress Detection in Geomaterials using K-band Frequency Modulated Continuous Wave Radar," *IEEE Access*, 2020, doi: 10.1109/ACCESS.2020.3002147.

[23] J. Blanche *et al.*, "Analysis of Sandstone Pore Space Fluid Saturation and Mineralogy Variation via Application of Monostatic K-Band Frequency Modulated Continuous Wave Radar," *IEEE Access*, 2018. https://ieeexplore.ieee.org/stamp/stamp.jsp?tp=&arnumber=8425025.

[24] O. Zaki *et al.*, "Self-Certification and Safety Compliance for Robotics Platforms," 2020.

[25] W. Tang, K. Brown, D. Flynn, and H. Pellae, "Integrity Analysis Inspection and Lifecycle Prediction of Subsea Power Cables," *PHM*. IEEE, pp. 105–114, 2018, doi: 10.1109/PHM-Chongqing.2018.00024.

[26] F. Dinmohammadi *et al.*, "Predicting Damage and Life Expectancy of Subsea Power Cables in Offshore Renewable Energy Applications," *IEEE Access*, vol. 7, pp. 54658–54669, 2019, doi: 10.1109/ACCESS.2019.2911260.

[27] M. G. Pecht and M. Kang, "PHM of Subsea Cables," *Prognostics and health management of electronics : Fundamentals, machine learning, and internet of things /*. Hoboken, NJ:, 2018, doi: 10.1002/9781119515326.

[28] J. H. Bradford and H. Marshall, "Estimating Complex Dielectric Permittivity of Soils from Spectral Ratio Analysis of Swept Frequency (FMCW) Ground-Penetrating Radar Data," *Am. Geophys. Union*.

[29] S. Rao and T. Instruments, "Introduction to mmwave Sensing: FMCW Radars." Accessed: Mar. 15, 2020. [Online]. Available: https://training.ti.com/sites/default/files/docs/mmwaveSensing-FMCW-offlineviewing_0.pdf.

[30] "Bridge Replacement Unit Costs 2019 - Bridge Tables - National Bridge Inventory - Bridge Inspection - Safety - Bridges & Structures - Federal Highway Administration." https://www.fhwa.dot.gov/bridge/nbi/sd2019.cfm.

[31] M. Barnes, S. Watson, D. Flynn, and S. Djurović, "Technology Drivers in Windfarm Asset Management," 2018.